



*Supplement of*

## **Remote sensing of aerosol water fraction, dry size distribution and soluble fraction using multi-angle, multi-spectral polarimetry**

**Bastiaan van Dierenhoven et al.**

*Correspondence to:* Bastiaan van Dierenhoven ([b.van.dierenhoven@sron.nl](mailto:b.van.dierenhoven@sron.nl))

The copyright of individual parts of the supplement might differ from the article licence.

## 1 Tables of daily statistics

For the 2020 winter and summer deployments of ACTIVATE and the 2019 CAMP<sup>2</sup>Ex campaign, daily averages of water fraction, dry effective radius and variance and number concentrations (for particles with  $D > 100 \mu\text{m}$ ) are shown in Table S1. Numbers in between brackets are standard deviations. Geometric averages and standard deviations are given for the number concentrations. In addition, the daily sulfate mass fraction derived from in situ observations and the soluble fraction retrieved by RSP are shown. Tables S2 and S3 gives the number of observations, observation time range and average latitude and longitude for the RSP and in situ data, respectively. In addition, table S2 shows daily averages and standard deviations of AOD, ambient effective radius and variance and refractive index retrieved by the RSP. Table S3 gives daily averages and standard deviations of the in situ-measured relative humidity,  $f(\text{RH})$ , derived  $\kappa$  values and the mass fraction of organics, ammonium and nitrate observed by the AMS. Note that the observed chloride fraction was always well below 1% and therefore not included.

5

10

Campaign	date	obs.	$f_w$	$r_{e,dry}$ [ $\mu\text{m}$ ]	$v_{e,dry}$	$N_a$ [ $\text{cm}^{-3}$ ]	$f_{m,sul}$ or $f_{sol}$
ACTIVATE winter 2020	28/02	I.S.:	0.23 (0.28)	0.12(0.03)	-	228(2.23)	0.29
		RSP:	0.23 (0.12)	0.17(0.02)	0.24(0.05)	128(1.43)	0.22
	29/02	I.S.:	0.14(0.18)	0.13(0.03)	-	264(4.77)	0.25
		RSP:	0.18(0.17)	0.15(0.02)	0.20(0.04)	299(1.26)	0.16
	01/03	I.S.:	0.15(0.23)	0.13(0.03)	-	251(3.43)	0.27
		RSP:	0.34(0.24)	0.17(0.02)	0.23(0.04)	170(1.38)	0.05
	09/03	I.S.:	0.29(0.29)	0.12(0.03)	-	178(2.66)	0.28
		RSP:	0.13(0.15)	0.14(0.02)	0.18(0.05)	176(1.37)	0.13
	11/03	I.S.:	0.27(0.22)	0.12(0.02)	-	429(2.38)	0.18
		RSP:	0.33(0.30)	0.15(0.01)	0.17(0.03)	125(1.48)	0.05
	12/03	I.S.:	0.39(0.25)	0.13(0.03)	-	199(4.17)	0.22
		RSP:	0.10(0.15)	0.15(0.02)	0.21(0.04)	263(1.65)	0.26
ACTIVATE summer 2020	17/08	I.S.:	0.41(0.25)	0.15(0.03)	-	101(2.98)	0.27
		RSP:	0.31(0.27)	0.16(0.03)	0.21(0.07)	296(1.66)	0.15
	20/08	I.S.:	0.33(0.14)	0.12(0.02)	-	686(1.86)	0.23
		RSP:	0.22(0.23)	0.16(0.02)	0.22(0.06)	375(1.59)	0.32
	21/08	I.S.:	0.42(0.13)	0.12(0.01)	-	367(4.07)	0.29
		RSP:	0.30(0.25)	0.17(0.02)	0.22(0.06)	292(1.57)	0.22
	02/09	I.S.:	0.19(0.09)	0.14(0.00)	-	595(1.21)	0.47
		RSP:	0.31(0.27)	0.15(0.02)	0.19(0.05)	268(1.59)	0.23
	23/09	I.S.:	0.07(0.10)	0.14(0.04)	-	406(2.45)	0.16
		RSP:	0.07(0.08)	0.17(0.01)	0.21(0.02)	283(1.30)	0.25
	29/09	I.S.:	0.21(0.23)	0.17(0.03)	-	119(3.08)	0.37
		RSP:	0.34(0.30)	0.15(0.03)	0.19(0.06)	186(1.45)	0.30
30/09	I.S.:	0.32(0.25)	0.13(0.03)	-	184(3.99)	0.30	
	RSP:	0.17(0.18)	0.17(0.02)	0.22(0.04)	171(1.35)	0.13	
CAMP <sup>2</sup> Ex 2019	27/08	I.S.:	0.54(0.20)	0.14(0.03)	-	166(4.50)	0.68
		RSP:	0.58(0.13)	0.14(0.02)	0.22(0.04)	258(1.41)	X
	30/08	I.S.:	0.26(0.20)	0.13(0.01)	-	376(2.10)	0.46
		RSP:	0.60(0.26)	0.15(0.01)	0.17(0.04)	357(1.39)	0.14
	04/09	I.S.:	0.19(0.22)	0.14(0.02)	-	486(3.33)	0.32
		RSP:	0.23(0.17)	0.17(0.01)	0.24(0.03)	267(1.21)	0.09
	06/09	I.S.:	0.20(0.18)	0.15(0.01)	-	747(3.50)	0.24
		RSP:	0.14(0.15)	0.16(0.01)	0.22(0.03)	573(1.24)	0.11
	08/09	I.S.:	0.15(0.15)	0.15(0.02)	-	233(3.36)	0.31
		RSP:	0.17(0.20)	0.15(0.02)	0.18(0.05)	242(1.28)	0.31
	13/09	I.S.:	0.50(0.30)	0.16(0.03)	-	264(4.57)	0.39
		RSP:	0.55(0.26)	0.13(0.02)	0.14(0.05)	176(1.77)	0.33
15/09	I.S.:	0.00(0.01)	0.18(0.02)	-	1092(6.42)	0.12	
	RSP:	0.02(0.03)	0.16(0.01)	0.26(0.03)	2406(1.53)	X	
16/09	I.S.:	0.15(0.25)	0.17(0.03)	-	442(6.03)	0.19	
	RSP:	0.29(0.28)	0.14(0.01)	0.20(0.04)	533(1.33)	X	
19/09	I.S.:	0.44(0.21)	0.14(0.02)	-	346(2.41)	0.66	
	RSP:	0.25(0.19)	0.21(0.03)	0.37(0.07)	310(1.18)	0.43	
21/09	I.S.:	0.33(0.17)	0.12(0.02)	-	568(2.16)	0.52	
	RSP:	0.40(0.19)	0.14(0.02)	0.21(0.04)	468(2.00)	0.62	
23/09	I.S.:	0.44(0.14)	0.13(0.01)	-	676(1.83)	0.61	
	RSP:	0.54(0.14)	0.12(0.01)	0.14(0.04)	495(1.30)	0.43	
27/09	I.S.:	0.61(0.23)	0.14(0.03)	-	73(1.63)	0.33	
	RSP:	0.62(0.35)	0.12(0.04)	0.13(0.05)	132(1.29)	X	
01/10	I.S.:	0.32(0.17)	0.15(0.01)	-	961(1.60)	0.46	
	RSP:	0.34(0.20)	0.13(0.02)	0.17(0.04)	644(1.77)	0.41	
03/10	I.S.:	0.32(0.14)	0.13(0.01)	-	833(3.19)	0.40	
	RSP:	0.38(0.24)	0.13(0.01)	0.22(0.03)	1045(1.52)	X	
05/10	I.S.:	0.50(0.27)	0.15(0.04)	-	84(4.14)	0.65	
	RSP:	0.51(0.24)	0.12(0.01)	0.17(0.02)	203(1.18)	X	

**Table S1.** Daily averages and standard deviations (within brackets) of RSP and in situ data (see text for details)

Campaign	date	$N_{obs}$	time [h]	lat.	lon.	AOD	$r_e$ [ $\mu\text{m}$ ]	$v_e$	refr.
ACTIVATE winter 2020	28/02	33	15.4-20.9	34.3	-73.8	0.07(0.01)	0.19(0.02)	0.26(0.05)	1.49(0.02)
	29/02	110	14.8-17.5	37.8	-73.4	0.15(0.06)	0.16(0.02)	0.22(0.05)	1.51(0.05)
	01/03	69	14.1-19.3	37.1	-74.1	0.08(0.03)	0.19(0.03)	0.27(0.07)	1.47(0.05)
	09/03	277	17.2-19.1	33.7	-74.6	0.06(0.03)	0.15(0.03)	0.19(0.05)	1.52(0.04)
	11/03	62	13.5-15.0	36.4	-72.3	0.10(0.03)	0.17(0.02)	0.22(0.06)	1.49(0.08)
	12/03	35	17.1-20.0	35.9	-75.2	0.13(0.04)	0.15(0.02)	0.21(0.03)	1.54(0.05)
ACTIVATE summer 2020	17/08	173	15.0-17.6	37.6	-72.7	0.17(0.10)	0.19(0.05)	0.27(0.10)	1.48(0.06)
	20/08	430	14.6-17.1	37.4	-73.4	0.20(0.11)	0.18(0.04)	0.24(0.08)	1.50(0.06)
	21/08	441	14.3-16.8	37.3	-72.2	0.22(0.11)	0.20(0.04)	0.27(0.08)	1.48(0.06)
	02/09	103	16.4-16.8	33.6	-74.4	0.12(0.07)	0.17(0.04)	0.22(0.07)	1.50(0.05)
	23/09	545	18.5-20.0	37.1	-72.3	0.32(0.13)	0.17(0.01)	0.20(0.03)	1.53(0.04)
	29/09	42	15.3-16.4	37.7	-70.7	0.14(0.11)	0.19(0.07)	0.25(0.09)	1.48(0.08)
30/09	340	16.4-19.3	38.0	-72.6	0.11(0.04)	0.19(0.03)	0.24(0.05)	1.51(0.05)	
CAMP <sup>2</sup> Ex 2019	27/08	30	4.0- 4.5	17.8	116.9	0.19(0.05)	0.19(0.03)	0.26(0.06)	1.42(0.04)
	30/08	35	26.9-27.8	8.3	119.6	0.19(0.05)	0.20(0.04)	0.27(0.08)	1.45(0.08)
	04/09	36	1.2- 1.6	9.3	117.7	0.14(0.03)	0.19(0.01)	0.29(0.05)	1.50(0.04)
	06/09	39	29.1-30.4	12.0	120.6	0.35(0.07)	0.17(0.02)	0.25(0.06)	1.52(0.04)
	08/09	15	26.7-26.8	18.5	123.3	0.12(0.04)	0.17(0.03)	0.23(0.05)	1.47(0.04)
	13/09	17	25.9-27.8	15.9	121.5	0.11(0.02)	0.18(0.02)	0.16(0.02)	1.49(0.03)
	15/09	43	27.0-28.8	9.1	119.4	0.84(0.15)	0.16(0.01)	0.25(0.04)	1.55(0.03)
	16/09	23	26.6-28.3	14.9	126.3	0.39(0.15)	0.17(0.02)	0.22(0.05)	1.53(0.06)
	19/09	24	29.7-29.9	18.2	122.6	0.32(0.05)	0.23(0.04)	0.37(0.08)	1.51(0.05)
	21/09	68	26.6-29.0	17.5	125.4	0.27(0.09)	0.17(0.02)	0.23(0.04)	1.48(0.06)
	23/09	100	24.7-26.8	17.8	126.1	0.19(0.05)	0.16(0.01)	0.21(0.02)	1.43(0.03)
	27/09	6	28.3-29.2	16.8	123.1	0.01(0.01)	0.21(0.02)	0.29(0.03)	1.47(0.01)
01/10	65	26.4-27.9	19.7	120.6	0.18(0.10)	0.16(0.02)	0.20(0.05)	1.48(0.05)	
03/10	16	24.8-25.0	14.0	120.5	0.23(0.07)	0.16(0.01)	0.24(0.02)	1.46(0.05)	
05/10	5	2.1- 2.8	15.4	123.9	0.06(0.04)	0.17(0.03)	0.22(0.05)	1.44(0.05)	

**Table S2.** Number of observations, observation time range and averages of latitude, longitude, effective radius, effective variance and refractive index retrieved by the RSP. Numbers in between brackets are standard deviations.

Campaign	date	$N_{obs}$	time [h]	lat.	lon.	RH [%]	f(RH)	$\kappa$	$f_{m,org}$	$f_{m,amm}$	$f_{m,nit}$
ACTIVATE winter 2020	28/02	3408	17.2-22.5	34.3	-73.3	72(17)	1.20(0.42)	0.12(0.18)	0.44	0.15	0.11
	29/02	7388	14.0-16.8	38.3	-72.4	70(13)	1.07(0.17)	0.05(0.05)	0.25	0.22	0.28
	01/03	3394	13.8-20.7	37.3	-73.1	66(16)	1.09(0.24)	0.06(0.09)	0.34	0.18	0.20
	09/03	4555	17.0-19.5	34.0	-74.8	70(19)	1.31(0.42)	0.15(0.19)	0.62	0.07	0.04
	11/03	7785	12.8-15.6	36.8	-73.4	81(9)	1.19(0.20)	0.09(0.09)	0.65	0.08	0.09
	12/03	10158	15.5-21.4	35.4	-73.6	81(9)	1.33(0.27)	0.15(0.12)	0.65	0.08	0.04
ACTIVATE summer 2020	17/08	5001	14.6-17.9	37.3	-72.8	84(7)	1.32(0.28)	0.15(0.13)	0.63	0.06	0.04
	20/08	1029	14.3-16.9	37.9	-73.1	67(12)	1.49(0.20)	0.23(0.10)	0.65	0.09	0.03
	21/08	1982	14.1-17.1	37.3	-73.1	70(7)	1.64(0.20)	0.30(0.10)	0.59	0.10	0.02
	02/09	264	15.8-15.9	35.7	-75.4	73(4)	1.20(0.12)	0.09(0.06)	0.43	0.08	0.02
	23/09	5776	18.0-20.2	37.1	-72.2	48(20)	1.09(0.16)	0.05(0.06)	0.72	0.08	0.03
	29/09	470	15.6-16.3	37.5	-70.9	69(16)	1.19(0.24)	0.10(0.10)	0.53	0.08	0.02
30/09	5806	16.4-19.5	37.6	-73.5	76(13)	1.29(0.26)	0.14(0.12)	0.57	0.09	0.04	
CAMP <sup>2</sup> Ex 2019	27/08	5219	2.6- 5.7	17.7	117.6	85(6)	1.46(0.27)	0.21(0.13)	0.22	0.09	0.01
	30/08	5973	25.3-28.9	8.4	119.7	78(11)	1.19(0.17)	0.09(0.07)	0.42	0.11	0.01
	04/09	790	0.2- 2.6	8.3	119.4	77(12)	1.09(0.16)	0.05(0.07)	0.57	0.09	0.02
	06/09	2695	27.9-31.9	15.1	119.4	85(3)	1.11(0.12)	0.05(0.05)	0.66	0.08	0.02
	08/09	2824	27.1-28.2	18.6	123.6	79(8)	1.09(0.17)	0.05(0.07)	0.61	0.06	0.02
	13/09	2871	24.9-28.2	17.9	121.7	85(8)	1.43(0.27)	0.20(0.12)	0.44	0.11	0.05
	15/09	4625	25.4-28.1	8.5	118.6	77(8)	0.92(0.05)	0.00(0.01)	0.79	0.06	0.02
	16/09	3091	25.2-26.1	14.3	125.4	82(5)	1.10(0.24)	0.06(0.11)	0.72	0.07	0.02
	19/09	6463	28.2-31.4	17.8	122.2	80(7)	1.41(0.19)	0.19(0.09)	0.22	0.10	0.01
	21/09	4281	25.0-30.5	16.1	124.8	73(12)	1.35(0.17)	0.16(0.08)	0.32	0.14	0.01
	23/09	2662	27.6-28.4	17.8	127.3	82(6)	1.36(0.10)	0.17(0.05)	0.22	0.15	0.01
	27/09	1627	26.7-27.4	22.3	125.1	90(2)	1.49(0.34)	0.23(0.16)	0.54	0.09	0.04
	01/10	7292	24.9-29.5	20.1	120.8	77(9)	1.26(0.11)	0.12(0.05)	0.37	0.15	0.02
03/10	5889	23.9-26.4	14.2	120.9	80(3)	1.27(0.16)	0.12(0.07)	0.43	0.12	0.05	
05/10	815	3.0- 4.1	15.8	125.2	86(4)	1.48(0.41)	0.23(0.19)	0.29	0.02	0.04	

**Table S3.** Number of observations, observation time range and averages of latitude, longitude, relative humidity, f(RH),  $\kappa$  and organics, ammonium and nitrate mass fractions obtained from in situ observations. Numbers in between brackets are standard deviations.

## 2 Uncertainties caused by the assumption of equal size distributions of the insoluble and dry soluble aerosol components

Here we estimate the uncertainties in inferred  $f_{sol}$ ,  $r_{e,dry}$  and  $v_{e,dry}$  caused by the assumption of equal size distributions of the insoluble and the dry soluble aerosol components. For this, we simulate  $r_{e,mix}$  and  $v_{e,mix}$  as a function of  $f_{sol}$  for a range of  $f_w$  and for an aerosol with a soluble component with  $r_{e,dry} = 0.15 \mu\text{m}$  and an insoluble component that is  $\Delta r_e$  smaller. For both components we assume  $v_{e,dry} = 0.15$ . For each combination of  $f_{sol}$ ,  $f_w$  and  $\Delta r_e$ , the dry values of  $r_{e,mix}$  and  $v_{e,mix}$  are calculated by first calculating the geometric mean and standard deviations and converting that to effective radius and variance used Eqs. 4 and 5. Furthermore,  $r_{e,mix}$  and  $v_{e,mix}$  are calculated for  $f_w > 0$ . We refer to these simulations as our 'dataset'. Similar simulations are made for the case with equal size distributions of the insoluble component and the dry soluble aerosol components, representing our 'look-up table'. To determine the bias caused by the equal insoluble and soluble size distributions, we use our look-up table to infer  $f_{sol}$ ,  $r_{e,dry}$  and  $v_{e,dry}$  from our dataset. For this, the variation of  $(v_{e,mix} + 1)/(v_{e,dry} + 1)$  with  $r_{e,mix}/r_{e,dry}$  for  $f_w > 0$  is determined from the simulations. Subsequently,  $f_{sol}$  is determined by finding  $f_{sol}$  in our look-up table for which the root mean squared differences of  $(v_{e,mix} + 1)/(v_{e,dry} + 1)$  as a function of  $r_{e,mix}/r_{e,dry}$  between the dataset and look-up table are smallest. Using the known  $f_w$ , Eqs. 20 and 21 are then used to infer  $r_{e,dry}$  and  $v_{e,dry}$ .

Resulting absolute biases in retrieved  $f_{sol}$  and relative biases in  $r_{e,dry}$  and  $v_{e,dry}$  are shown in Fig S1. For a  $\Delta r_e$  of  $0.03 \mu\text{m}$ , maximum underestimations of  $f_{sol}$ ,  $r_{e,dry}$  and  $v_{e,dry}$  are 0.23, 9% and 17%, respectively, occurring at true  $f_{sol}$  values of 0.65, 0.28 and 0.16, respectively. For  $f_{sol}$  greater than about 0.6,  $v_{e,dry}$  is overestimated by 4% at maximum. These biases scale approximately linearly with  $\Delta r_e$ , although the values of  $f_{sol}$  where maximum biases occur somewhat varies with  $\Delta r_e$ .

## 3 Refractive indices of binary aqueous mixtures of organics and ternary mixtures with organics and inorganic salts.

Here we analyze refractive indices of binary aqueous mixtures of organics and ternary mixtures with organics and inorganic salts as a function of volume water fraction. Refractive index and density data is obtained from Lienhard et al. (2012) (their Table 5). Figure S2 shows refractive indices for aqueous mixtures of levoglucosan and three aqueous mixtures of both levoglucosan and 1) ammonium sulfate, 2) ammonium nitrate and 3) ammonium bisulfate as a function of volume water fraction. In the ternary mixtures, the molar ratio of levoglucosan and salts were 1:1. The original data is given as a function of mass fraction of solute ( $f_{m,s}$ ). Here we convert

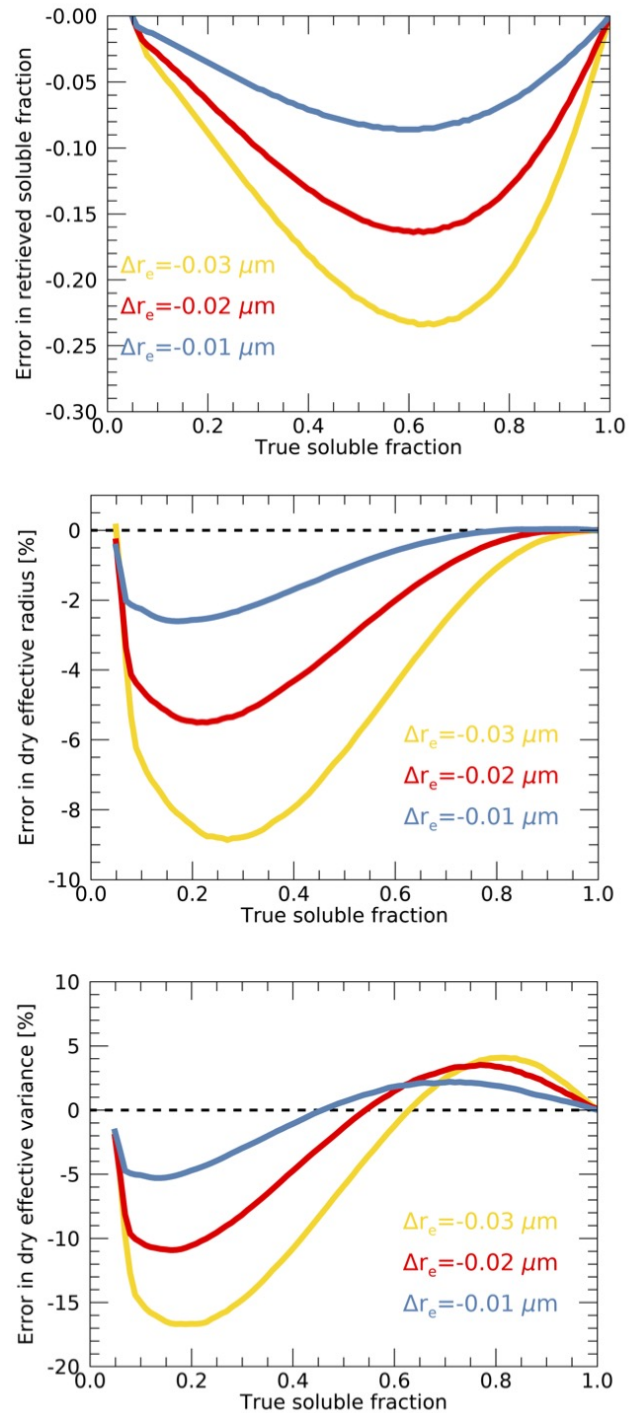


**Figure S1.** Estimated uncertainties in inferred  $f_{sol}$  (top),  $r_{e,dry}$  (middle) and  $v_{e,dry}$  (bottom) caused by the assumption of equal size distributions of the insoluble and the dry soluble aerosol components. Differences  $\Delta r_e$  between effective radius for dry soluble aerosol and insoluble are assumed to be 0.01 (blue), 0.02 (red) and 0.03 (yellow)  $\mu\text{m}$ .

those fractions to volume water fractions ( $f_w$ ) through

$$f_w = 1 - f_{m,s} \frac{\rho_{mix}}{\rho_{dry}}, \quad (1)$$

where  $\rho_{mix}$  is the density of the binary or ternary aqueous mixture given by Lienhard et al. (2012) and  $\rho_{dry}$  is the refractive index of the dry particles. For the mixtures with ammonium nitrate and ammonium bisulfate,  $\rho_{dry}$  is taken as the values at  $f_{m,s} = 1$  provided by Lienhard et al. (2012). For the other mixtures, mass fractions close to unity were reported by Lienhard et al. (2012) and here we obtain densities at  $f_{m,s} = 1$  by linear extrapolation. Also given in Fig. S2 (dashed lines) are the refractive indices obtained using the volume mixing rule. A linear least-squares fit through the data is used to obtain the dry refractive indices for those mixtures that did not extend all the way to  $f_{m,s} = 1$  in the Lienhard et al. (2012) dataset. It can be seen that the volume mixing approach performs well in these cases of organic aerosol and ternary mixtures containing organic aerosol and inorganic salts. Similar results are obtained for other binary aqueous mixtures of organics reported by Lienhard et al. (2012). For reference, the refractive index of pure ammonium sulfate as provided by Tang and Munkelwitz (1991) is also given in Fig. S2 (red line). Here a dry density of  $1.76 \text{ g/cm}^3$  is used (Erlick et al., 2011) to convert  $f_{m,s}$  to  $f_w$  using Eq. 1. Note that this line is only plotted up to the critical mass fraction at which efflorescence occurs, assumed to be  $f_{m,s} = 0.8$ .

#### 4 Effective refractive indices of external mixtures.

Remote sensing observations as presented in the main text, as well as in situ light scattering probes yield the effective refractive index of the observed population of aerosol particles, which may be externally mixed with several modes. A reasonable assumption may be that the effective refractive index is the optical depth-weighted average of those of the separate modes. In turn, as fine mode aerosol extinction roughly scales with its volume, the volume mixing rule may yield a good approximation of the effective refractive index of external mixtures. To test this assumption, we calculate the single scattering properties of an external mixture of two aerosol modes with different refractive indices and then determine the refractive index of a single mode aerosol that is radiatively most equivalent to the external mixture, which can be considered as the effective refractive index of the mixture.

For this approach, Mie calculations are performed to calculate the phase matrices of non-absorbing aerosol modes with varying refractive indices. Subsequently, the phase matrices of two modes are added, weighted by the volume fractions and volume scattering efficiencies. The  $P_{12}$  element of the phase matrix is divided by the  $P_{11}$  element to obtain the degree of linear polarization (DoLP). A radiatively equivalent single mode aerosol is then retrieved by finding the low-

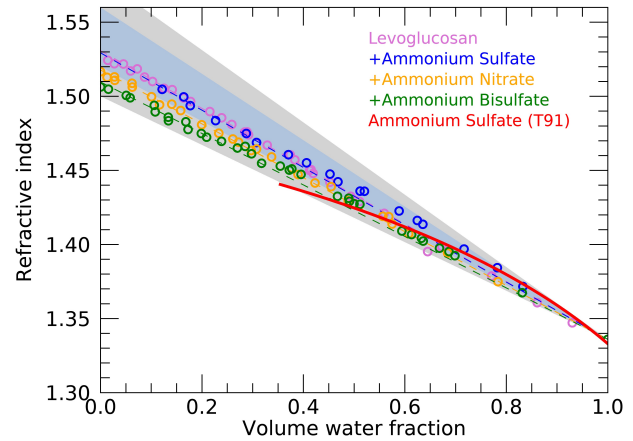


**Figure S2.** Refractive mixture of binary solutions of levoglucosan and water and three ternary solutions of levoglucosan, water and inorganic salts, as indicated by the different colors. Dots are derived from observations of Lienhard et al. (2012), while dashed lines are approximations using the volume mixing rule. The red line represents the parameterized refractive index of pure ammonium sulfate provided by Tang and Munkelwitz (1991). Blue and grey areas are ranges obtained by applying the volume mixing rule to  $n_{dry} = 1.54 \pm 0.02$  and  $n_{dry} = 1.54 \pm 0.04$ , respectively.

est root-mean-squared difference (RMSD) between the scattering properties (i.e.  $P_{11}$  and DoLP) of the external mixture and that of a single mode of which the refractive index is varied. Here, the RMSD is calculated for scattering angles between  $90^\circ$  and  $165^\circ$ .

To focus only on the real part of the refractive index, the size distribution is the same for both modes in the mixture and the single mode assumed for the effective refractive index retrieval, with a effective variance of 0.2 and effective radii of 0.12, 15, or 0.18  $\mu\text{m}$ . One of the modes is assumed to have an refractive index of 1.54, while the refractive index of the second mode is varied between 1.33 and 1.54. These modes may be interpreted as respectively a insoluble mode and a soluble mode with a water fraction ranging from zero to unity assuming a volume mixing rule (cf. main text). The effective refractive index of the external mixture estimated using the volume fraction mixing rule is compared with the retrieved effective refractive index to assess the accuracy of using volume fraction mixing for the interpretation of the retrieved effective refractive index. Here, we focus on an equal fraction of the two modes (i.e.,  $f_{mode1} = 0.5$ ), since the maximum errors are expected for that case.

Figure S3 shows the differences between the estimated refractive index according to volume fraction mixing and that of the radiatively equivalent single mode aerosol. Volume mixing is shown to mostly underestimate the effective refrac-

tive index of the mixture. The absolute errors are shown to decrease as the difference between the refractive indices of the two modes decreases. Furthermore, the error depends on effective radius with largest errors for the small sizes. This behavior can be explained by the variation of the scattering efficiencies with size and refractive index, i.e. the error in the effective volume mixing refractive index increases as the difference in scattering efficiency of the two modes increases.

The errors in effective refractive index from assuming the volume mixing are relatively large at 0.035, 0.026 and 0.018 for the extreme case with an equal mixture of a purely dry aerosol mode and purely water aerosol mode, for effective radii of 0.12, 15, and 0.18  $\mu\text{m}$ , respectively. In this case, the total volume water fraction estimated from the total refractive index under the assumption of the volume mixing rule would be 0.17, 0.13 and 0.09, respectively. However, we stress that these uncertainties must be considered as maximum values. For example, for an equal mixture of a purely dry aerosol mode and an aerosol mode containing 85% water (with refractive index of 1.365), errors in effective refractive index drop to 0.021, 0.013 and 0.006 for the three sizes, respectively, with representative errors in retrieved water volume fraction of less than 0.10, 0.06 and 0.03 for the three sizes, respectively. Furthermore, errors further decrease for mixing fractions deviating from 0.5. Hence, we can reasonably assume that the effective refractive index retrieved using multi-angle polarimetry is generally within about 0.02 of the volume-weighted refractive index of the externally mixed aerosol. Moreover, for our purpose of inferring volume water fraction from the retrieved effective refractive indices, the mixing state of the aerosol is generally irrelevant.

## References

- Erlick, C., Abbatt, J. P. D., and Rudich, Y.: How Different Calculations of the Refractive Index Affect Estimates of the Radiative Forcing Efficiency of Ammonium Sulfate Aerosols, *Journal of Atmospheric Sciences*, 68, 1845–1852, <https://doi.org/10.1175/2011JAS3721.1>, 2011.
- Lienhard, D. M., Bones, D. L., Zuend, A., Krieger, U. K., Reid, J. P., and Peter, T.: Measurements of Thermodynamic and Optical Properties of Selected Aqueous Organic and Organic–Inorganic Mixtures of Atmospheric Relevance, *The Journal of Physical Chemistry A*, 116, 9954–9968, <https://doi.org/10.1021/jp3055872>, pMID: 22974307, 2012.
- Tang, I. N. and Munkelwitz, H. R.: Simultaneous Determination of Refractive Index and Density of an Evaporating Aqueous Solution Droplet, *Aerosol Science and Technology*, 15, 201–207, <https://doi.org/10.1080/02786829108959527>, 1991.

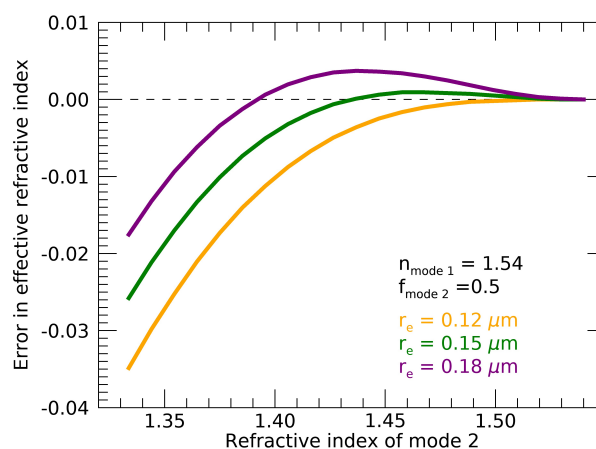


**Figure S3.** Error in effective refractive index of a two-mode aerosol mixture from applying the volume fraction mixing rule as a function of the refractive index of one of the modes. The other mode is assumed to have a refractive index of 1.54. An equal fraction of the two modes is assumed. Results are shown for aerosols with size distributions with a effective radius of 0.12 (orange), 0.15 (green) and 0.18 (purple)  $\mu\text{m}$ .